Isotopic shift, pressure shift, and pressure broadening of the $7d'$ states of neon using Doppler-free two-photon absorption spectroscopy

M. M. Salour

Department of Physics and Gordon McKay Laboratory, Harvard University, Cambridge, Massachusetts 02138
(Received 5 August 1977)

Doppler-free two-photon transitions between the $3s$, $J = 2$ metastable state and the subconfiguration $7d'$ of neon are studied with a pulsed-dye-laser oscillator-amplifier system which was synchronized with a chopped rf discharge in neon vapor. The isotopic shifts for these transitions are measured, and based on these measurements we have made a systematic study of Ne-Ne and Ne-He collisional broadening and shift of these very narrow Doppler-free two-photon resonances.

I. INTRODUCTION

With the introduction of powerful, narrow-band tunable lasers as sources of intense monochromatic light, it has recently become possible to perform high-resolution spectroscopy of atomic and molecular states which are not directly coupled to the ground state via an electric dipole matrix element. These modern methods of precision spectroscopy have thus far combined stepwise excitation of atoms and molecules by tunable dye lasers with level-crossing techniques,[1] quantum beat spectroscopy,[2] optical double resonance,[1] or Doppler-free two-photon absorption spectroscopy.[3] In particular, using the Doppler-free-two-photon technique, it has recently been possible to measure fine and hyperfine structures, and to study Zeeman and Stark splittings and collision effects. While most of these investigations were performed in alkali vapors (in particular, sodium), there has been considerable interest in extending these measurements to rare-gas atoms,[4] whose levels are spread over a wide range in energy so that one can often find a level among them as an intermediate state to enhance the two-photon transition probability. Neon in particular has a very interesting energy-level structure which makes it attractive for two-photon spectroscopy. This may easily be shown by comparing the energy-level diagrams of sodium and neon. If neon atoms are somehow excited into either of the metastable $2p^5 3s$, $J = 2$ or $2p^5 3s$, $J = 0$ states, then either of these states could serve as a starting point for performing many experiments in neon vapor identical to those previously performed in sodium, without any major change in experimental configuration. Another interesting feature of neon is that it has three stable isotopes, ^{20}Ne, ^{21}Ne, and ^{22}Ne; thus one may explore interesting effects resulting from the presence of different isotopes in a vapor cell.

II. FORMALISM

For the excited states of neon in a $2p^5 nl (n \geq 4)$ configuration, the various terms of the Hamiltonian can be ordered in the following way[5]:

$$\mathcal{H}_{SO}(\text{core}) \gg \mathcal{H}^d_{elec}(\text{core-external elec.})$$

$$\gg [\mathcal{H}^e_{elec}(\text{core-external elec.})$$

$$\text{and } \mathcal{H}_{SO}(\text{external elec.})]. \tag{1}$$

The spin-orbit (SO) coupling Hamiltonian of the $2p^5$ core, $\mathcal{H}_{SO}(\text{core})$, is larger than the direct electrostatic interaction between the core and the external electron, $\mathcal{H}^d_{elec}$; the latter is itself larger than the exchange part of the electrostatic interaction, $\mathcal{H}^e_{elec}$, and the spin-orbit interaction of the external electron, $\mathcal{H}_{SO}(\text{external electron})$. To find the eigenstates of the Hamiltonian, one can apply stationary-state perturbation theory. $\mathcal{H}_{SO}$ (core) is invariant under any rotation of core variables; hence the eigenstates of this term of the Hamiltonian are eigenstates of $\vec{j}_1$, where $\vec{j}_1$ is the angular momentum of the core,

$$\vec{j}_1 = \vec{L}_1 + \vec{S}_1, \tag{2}$$

where $\vec{L}_1$ and $\vec{S}_1$ are the orbital angular momentum and spin, respectively, of the core.

The angular momenta of the $2p^5$ core are $L_1 = 1$, $S_1 = \frac{1}{2}$. Thus j_1 can take the two values $\frac{1}{2}$ and $\frac{3}{2}$. Levels for which $j_1 = \frac{1}{2}$ will be indicated with primes. The levels of the $2p^5 nl' (j_1 = \frac{1}{2})$ subconfiguration have a larger energy than the levels of the $2p^5 nl (j_1 = \frac{3}{2})$ subconfiguration because the fine structure of the core is inverted (as a consequence of the Racah theorem[5]). One can interpret this intuitively by saying that the core behaves as a positively charged hole.

When the direct part of the electrostatic interaction between the core and the external electron is taken into account, the Hamiltonian is only invariant under a rotation of the core and of the or-

bital variables of the external electron. Under these conditions, the eigenstates of the Hamiltonian are eigenstates of

$$\vec{k} = \vec{j}_1 + \vec{l}, \qquad (3)$$

where $\vec{l}$ is the orbital angular momentum of the external electron. Under these conditions, the eigenstates of the Hamiltonian are no longer exact eigenstates of j_1, since the electrostatic interaction can couple levels of different j_1. Nevertheless, as long as condition (1) is fulfilled, j_1 remains a good quantum number to a very good approximation. When the electrostatic interaction and the core spin-orbit coupling are of the same order of magnitude, which is the case in the $2p^5 3p$ configuration, j_1 is no longer a good quantum number, while k is a good quantum number.

When the exchange term of the electrostatic interaction and the spin-orbit coupling of the external electron are taken into account, the Hamiltonian is invariant only under an overall rotation of the orbital and spin variables, and only the total angular momentum J of the electrons is a good quantum number:

$$\vec{J} = \vec{k} + \vec{s}, \qquad (4)$$

where $\vec{s}$ is the spin of the external electron.

Taking condition (1) into account, however, j_1 and k are good quantum numbers to within a reasonable approximation (however, Liberman has shown[6] that for $J \geq 2$, k is no longer a reasonably good quantum number), and we will find later that the eigenstates of the Hamiltonian differ only slightly from $|(L_1, S_1), (j_1, l), (k, s), J, M_J\rangle$. For convenience, we write these states as $|nl[k], J, M_J\rangle$ or $|nl'[k], J, M_J\rangle$, depending on whether j_1 is equal to $\frac{3}{2}$ or $\frac{1}{2}$. This is called Racah or j-l coupling.

In our experiment we studied the subconfiguration $7d'$ of neon. This subconfiguration consists of four levels, which, according to the Paschen notation, are written in the following forms: $7s_1'$, $7s_1'''$, $7s_1''''$, and $7s_1''$ (in order of decreasing energy). They are also designated by their Racah coupling scheme:

$$7s_1' \simeq 7d'[\tfrac{3}{2}], \quad J=1; \quad 7s_1''' \simeq 7d'[\tfrac{5}{2}], \quad J=3;$$

$$7s_1'''' \simeq 7d'[\tfrac{5}{2}], \quad J=2; \quad 7s_1'' \simeq 7d'[\tfrac{3}{2}], \quad J=2.$$

We used the metastable $2p^5 3s$ ($J=2$) state as the initial state, although the metastable $2p^5 3s$ ($J=0$) state could equally well have been used. It happens that for transitions leading to the configuration $2p^5 7d'$, a slightly longer wavelength laser photon is needed if the $2p^5 3s$ ($J=0$) is used as the initial state.

III. EXPERIMENTAL

In order to excite the neon atoms to either of the metastable states, one must make an electrical discharge in the neon cell. For this we used a model C201 Epsco rf generator with a model 1403H plug-in head. After many unsuccessful attempts to find two-photon transition signals, it was realized that the noise level due to spontaneous emission of atoms excited in the rf discharge was high enough to completely obscure the fluorescence emitted by atoms excited by laser photons. Thus it became necessary to chop the rf discharge and monitor the fluorescence in the afterglow. The problem becomes a bit more complicated when a pulsed laser is employed, because it is then necessary to synchronize the chopped rf discharge with the pulsed dye laser.

The synchronization scheme used in our experiment is illustrated in Fig. 1. A 1-kHz crystal oscillator, generating square waves, was amplified to 55 V to externally trigger the rf discharge generator. Meanwhile, because it was not possible to trigger the nitrogen laser at a repetition rate of 1 kHz, two model 7490 integrated circuit chips were used to set the repetition rate of the N_2 laser at 10 pulses/sec (each chip divided the repetition rate by ten). Thus atoms in the neon cell were excited by the 0.5-msec-long rf discharge pulses. The lifetimes of the two metastable states are on the order of a few msec, while the lifetimes of the higher excited states are in the 10^{-9} to 10^{-6} sec range. In order to eliminate spontaneous radiation from the higher excited states, an adjustable delay was introduced so that once atoms were excited into the metastable state, a delay of a few microseconds would occur before the laser was triggered. During this few microsecond delay, practically all atoms in the higher excited states would decay; when the laser was suddenly triggered after this delay, it would pump atoms from the
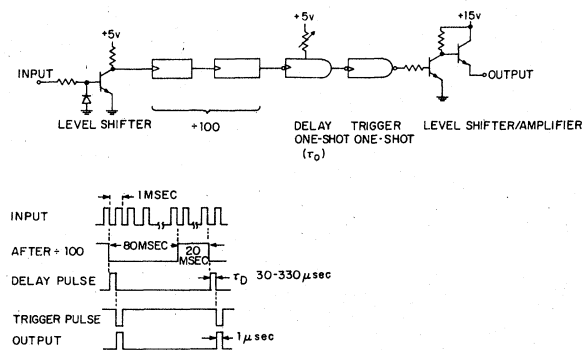
FIG. 1. Schematic for synchronization of chopped rf discharge with pulsed N_2 laser.
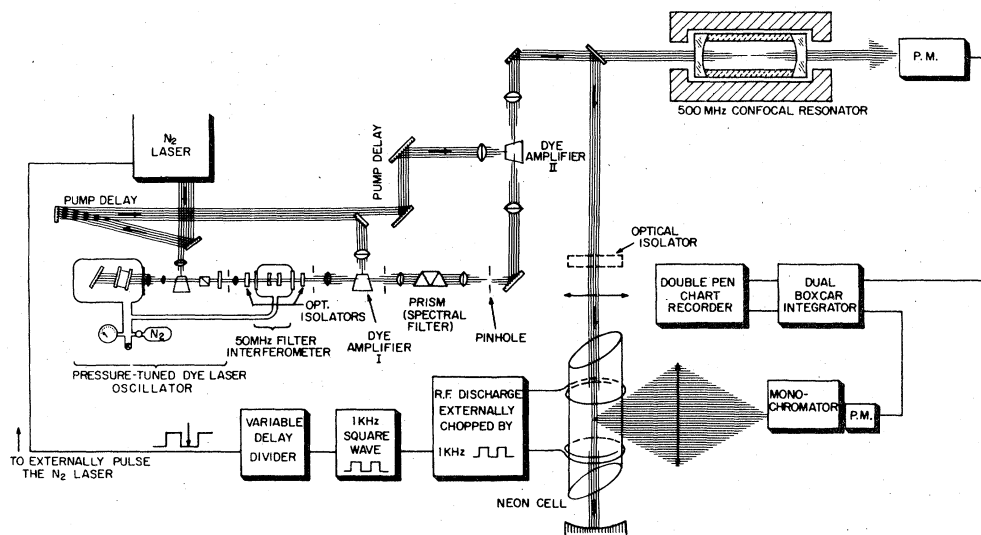
FIG. 2. Experimental arrangement for the measurement of isotopic shifts.

populated metastable state to the desired excited state.

In practice, the number of atoms excited to the metastable state by the discharge did not depend upon the neon pressure. The only noticeable effect of raising the neon pressure was the broadening and shift of the absorption lines, a phenomenon which is discussed later in this paper.

Figure 2 shows our experimental arrangement.
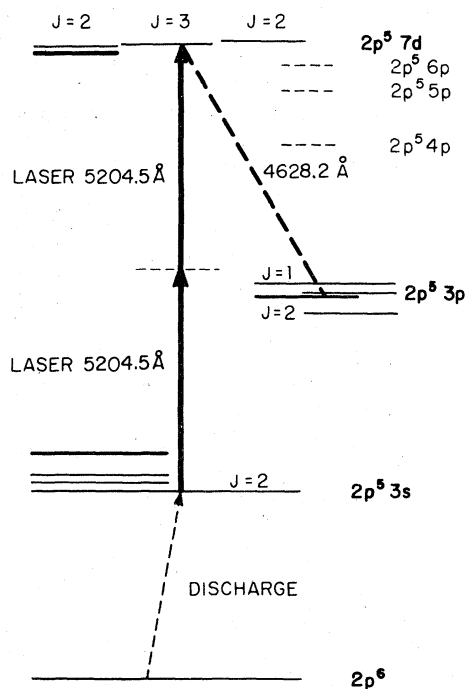
FIG. 3. Simplified energy-level diagram.

A narrow-band pressure-tuned dye laser oscillator with a confocal filter interferometer, followed by two stages of dye amplifiers pumped by the same nitrogen laser,[7] was employed. The nitrogen laser was externally triggered and synchronized with the chopped rf discharge. Part of the output of the second-stage dye amplifier was focused into a 15-cm-long confocal interferometer for frequency calibration, but the larger part was focused into the neon cell. The radiation transmitted through the cell was reflected back and refocused into the neon cell to provide the second beam required for the Doppler-free two-photon technique. The fluorescence produced by the decay of excited neon atoms was collected and analyzed. The desired wavelength of the fluorescence was selected by a monochromator and the intensity was measured with a model EMI 9658 R photomultiplier. The average heights of the pulses produced by the photomultiplier monitoring the fluorescence, and by the other photomultiplier monitoring the frequency calibration with the confocal interferometer, were independently analyzed by a dual channel boxcar integrator. The result was recorded by a double-pen chart recorder.

IV. PHYSICAL DISCUSSION AND EXPERIMENTAL RESULTS

Figure 3 shows the simplified energy-level diagram in our experiment. Note that the metastable state $2p^53s$ $(J=2)$ is a pure Racah state of $j_1 = \frac{3}{2}$, while the states of configuration $7d'$ differ slightly from pure Racah states with $j_1 = \frac{1}{2}$. The transitions between these different j_1 levels are possible, first, because the fine structure of the interme-

diate $2p^53p$ states is larger than the energy deficit $\hbar\Delta\omega_r = \hbar(\omega_L - \omega_r)$, and second, because these levels are not pure Racah states, since the electrostatic interaction is comparable to the spin-orbit coupling of the core. In our experiments, the predominant intermediate levels, corresponding to the smallest values of the energy deficit $\hbar\Delta\omega_r$, are $2p_2$ ($J=1$), $2p_4$ ($J=2$), and $2p_5$ ($J=1$). Note that the level $2p_3$ ($J=0$) also corresponds to a small $\hbar\Delta\omega_r$, but an electric dipole transition cannot be induced between the metastable state $2p^53s$ ($J=2$) and this level $2p_3$ ($J=0$). In the case of the $7s'''(J=3)$ state, the level $2p_4$ ($J=2$) alone among the three levels mentioned above can play a role as an intermediate level.

In our experiments we made a considerable effort to observe the two-photon transitions leading to the $7s_1'$ ($J=1$) level. Unfortunately, because this level is coupled to the ground state $2p^61s_0$ by the electric dipole Hamiltonian, the fluorescence was practically self-trapped by the emission of a far uv photon, which was impossible to detect through the windows of the cell. One way to avoid this difficulty would be to increase the signal of the $3s[\frac{3}{2}]2$-$7d'[\frac{3}{2}]1$ two-photon transitions by placing the neon cell inside a Fabry-Perot interferometer which is locked to the laser frequency, and then observing the $7s_1' \rightarrow 2p_2$ fluorescence at 4666.6 Å. This technique was first suggested and applied to the $4d'[\frac{3}{2}]1$ level of neon by Biraben and co-workers.[8] In our experiments, instead, we concentrated on the study of collisional shifting and broadening of the other three levels, a phenomenon which was of more interest to us, and will be discussed later in this paper.

As illustrated in Fig. 3, the two-photon resonances were detected by using a monochromator to monitor the fluorescence from the excited $7d'$ state to the intermediate p states. For the $7s_1'''$, $7s_1''''$, and $7s_1''$ levels, we detected the following fluorescence lines, respectively:

$7s_1'''-2p_4$ at 4628.2 Å,

$7s_1''''-2p_5$ at 4609.8 Å,

$7s_1''-2p_2$ at 4667.3 Å.
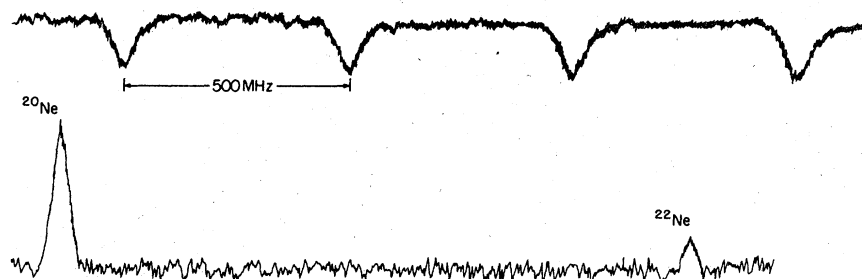
One can calculate the number of excited atoms in any of the $7d'$ subconfiguration levels produced by two-photon excitation, and compare it with the equivalent $3^2S \rightarrow 7^2D$ two-photon excitation in sodium. Such comparison reveals[9] that with equal laser intensity, the probability of two-photon absorption is slightly smaller for neon than for sodium.

For the levels $7s_1''$ ($J=2$), $7s_1'''$ ($J=3$), and $7s_1''''$ ($J=2$), isotopic shifts between two-photon absorption lines corresponding to isotope 20 and to isotope 22 were measured. Figure 4 shows a typical experimental trace of a two-photon transition in neon vapor. The two peaks correspond to the same transition in the even isotopes ^{20}Ne and ^{22}Ne. The intensity of these two peaks is proportional to the natural abundance of each isotope (neglecting the pulse-to-pulse jitter of the dye laser; these signals were not normalized to the square of the laser intensity). In order to measure this isotopic shift with high precision, these observations must be repeated many times to reduce the statistical error. If the entire laser frequency range is scanned slowly, these measurements will be very time-consuming. We later discovered that it is sufficient to scan slowly in the beginning over at least one free spectral range (two peaks) of the confocal resonator, around one of the peaks of the two photon resonances, then to sweep more rapidly in the region which separates the two resonances, while counting the number of peaks of the confocal resonator. This technique can save a good deal of time in data taking, especially when a longer confocal resonator (with a smaller free spectral range) is used, in which case the peaks of the frequency marker are closer together. From these recordings we have measured the isotopic shift between ^{20}Ne and ^{22}Ne in the three subconfiguration levels of $7d'$. The results are presented in Table I. Note that these values are more or less the same; the statistical uncertainty and the linewidth of the laser did not allow us to differentiate among them. Also note that these values correspond to twice the laser frequency illustrated in Fig. 4.

The experimental results presented here could be extended to almost all levels of neon that can

^{20}Ne

$\longmapsto$ 500 MHz $\longmapsto$

^{22}Ne

FIG. 4. Typical experimental trace: $1s_5(J=2)$-$7s_1''(J=3)$ two-photon transitions.

TABLE I. Isotopic shifts, Ne–Ne collisional broadenings and shifts, and He–Ne collisional broadenings and shifts, in three levels of subconfiguration $7d'$ of neon.

Two-photon transition	$\Delta v = v(^{22}\text{Ne}) - v(^{20}\text{Ne})$	Ne–Ne collision broadening (MHz/Torr)	Ne–Ne pressure shift (MHz/Torr)	He–Ne collision broadening (MHz/Torr)	He–Ne pressure shift (MHz/Torr)
$\Delta v[1S_5 \rightarrow 7S''_1 \ (J=2)]$	2796 ± 10 MHz	42 ± 8	-10 ± 4	59 ± 10	6 ± 3
$\Delta v[1S_5 \rightarrow 7S'''_1 \ (J=3)]$	2797 ± 8 MHz	43 ± 7	-8 ± 3	58 ± 12	5 ± 2
$\Delta v[1S_5 \rightarrow 7S''''_1 \ (J=2)]$	2799 ± 9 MHz	41 ± 7	-8 ± 4	60 ± 12	7 ± 4

be excited from any of the metastable states with our pulsed dye laser oscillator-amplifier system. Our purpose in this paper is to demonstrate that very narrow Doppler-free two-photon resonances can be used for the study of isotopic shifts in atomic vapors without great difficulty. It is interesting to note that since Bohr's shift varies as

$$1/M_1 - 1/M_2 \simeq \Delta/M^2 \, ,$$

(where $\Delta = M_2 - M_1$ is on the order of a few units), while the Doppler width only decreases as $1/\sqrt{M}$, the isotopic shift (which in the case of neon turns out to be of the same order of magnitude as the Doppler width) will be smaller than the Doppler width for heavier elements. This reasoning is not entirely correct, since the isotopic shift does not vary monotonically with increasing Z because of the specific shift. Moreover, for heavier elements one must take into account the volume shift. However, it is highly probable that the method of Doppler-free two-photon spectroscopy can provide a good deal of important information about isotopic shifts in elements heavier than neon.

V. STUDY OF COLLISIONS

While most of the initial interest in Doppler-free two-photon spectroscopy has centered on the achievement of higher resolution spectra, there have been some attempts to use this technique as a probe of collisonal processes occurring within atomic and molecular systems.[10] The effects of internal collisions on absorption and emission lines associated with atomic and molecular systems have traditionally been referred to as "pressure broadening." Pressure-broadening theories allow the experimenter to fit an observed line shape to some predicted formula, and, by so doing, (i) obtain characteristic collision parameters associated with the experimental system, and (ii) determine the zero-pressure limit of the data, which, among other things, might yield atomic- or molecular-state lifetimes. In principle, standard spectroscopy should provide the proving ground for pressure-broadening theories. In practice, however, despite the fact that pressure-broadening theories have existed since the early 1900's, substantial progress has not been made in testing the validity of various theories. This is due in part to the fact that simple rate constants which depend linearly on the pressure have been fairly successful in accounting for pressure effects. More importantly, the large Doppler width associated with atomic or molecular systems has masked subtle collision effects.

Thus very narrow Doppler-free resonances can provide the means to obtain both qualitative and
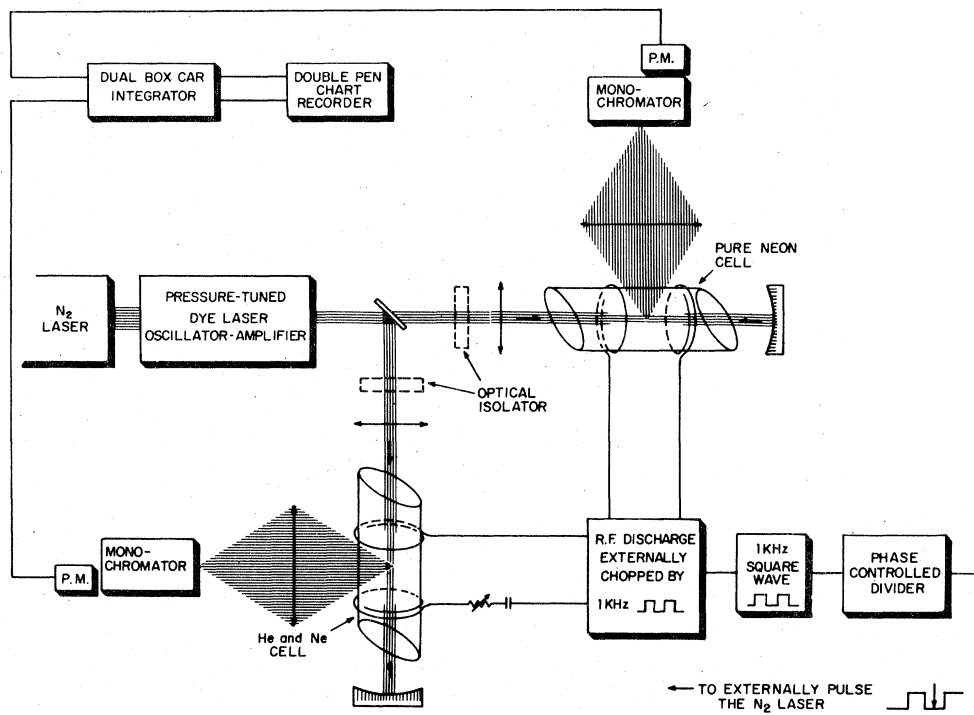
FIG. 5. Experimental arrangement for the study of collision effects.

quantitative data for collisions involving either excited- or ground-state atoms. Doppler-free techniques permit the measurement of the broadening and shift of a spectral line due to collisions as well as the determination of other relaxation parameters, such as collisional quenching rates, rates of collisional relaxation of magnetic substates, velocity thermalization rates, and collision kernels, which manifest themselves in the line shapes associated with atomic and molecular systems. The determination of these parameters is important not only for the correct interpretation of experiments where collisions play a role, but also because the parameters provide clues about the nature of the interatomic potential giving rise to the relaxation; furthermore, they allow a more sensitive measure of the manner in which collisions perturb the energy levels and alter the velocity of the active (emitting or absorbing) atoms.

Figure 5 illustrates the experimental arrangement used to study the collisional shift and broadening of the levels of neon in subconfiguration $7d'$, whose isotopic shifts were measured previously.

The 60 kW output of the pressure-tuned pulsed dye laser oscillator-amplifier system was split into two parts. The first part was focused into a reference neon cell, normally at 0.4 Torr of neon pressure, and the remainder was focused into a sample neon cell which was filled with either neon or a one-to-one mixture of helium and neon at higher pressures.

Both cells were placed in a laser standing-wave field; they were simultaneously exposed to a discharge from an rf discharge system, which was chopped and synchronized with the pulsed dye laser system as described earlier. The fluorescence signals produced after the two-photon excitations in each cell were collected and analyzed. The relevant wavelength of the fluorescence in each cell was selected by a monochromator, and its intensity was measured by a model EMI 9658 R photomultiplier. The average heights of the pulses produced by the two photomultipliers monitoring the fluorescence signals from the two cells were simultaneously and independently analyzed by a dual-channel box-car integrator, and the results were simultaneously recorded by a double-pen chart recorder.

Figure 6 illustrates typical traces obtained for the case of neon-neon collisions; they clearly indicate broadening of the resonance lines. A careful examination of these traces also indicates that the resonances are shifted towards the red side of the spectrum.

Table I also gives the neon-neon collisional broadenings and shifts of the three levels of subconfiguration $7d'$ of neon. These results correspond to the ^{20}Ne line. The ^{22}Ne line was much weaker, and an accurate measurement of its
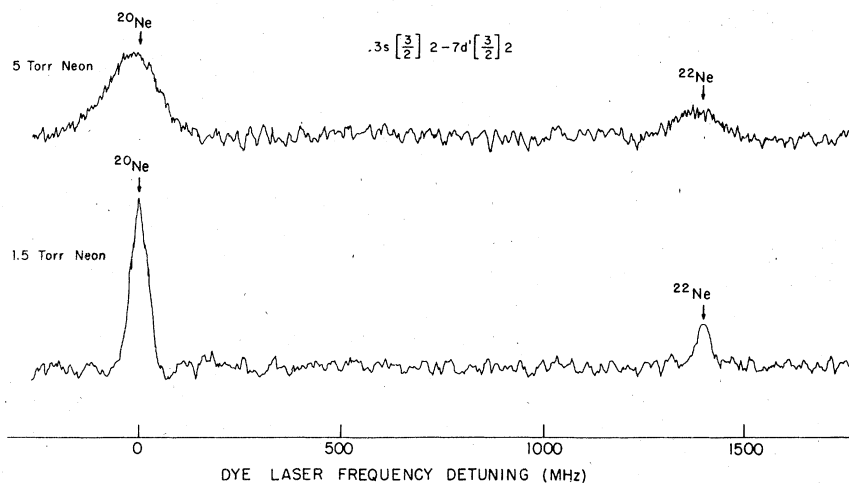
FIG. 6. Typical experimental trace for Ne-Ne collisions. The upper trace corresponds to the sample cell; the lower trace corresponds to the reference cell.

broadening and shift parameters was difficult. Neglecting the experimental uncertainties, the broadenings and shifts are almost identical for the three transitions considered. Had our laser linewidth been narrower, it would have been possible to reduce the experimental uncertainty somewhat, perhaps making it possible to distinguish among the broadenings and shifts of the three levels.

Figure 7 illustrates typical traces obtained for helium-neon collisions. In contrast to the Ne-Ne collision process, He-Ne collisions caused a blue shift in the broadened resonance lines. The He-Ne collisional broadenings and shifts of these three subconfiguration levels are also given in Table I.

These measurements of the relative shift and broadening of the two-photon resonances may be used to determine the atomic interaction potential. In particular, when studying the broadening and shift of these lines resulting from collisions with foreign gases, it would be particularly interesting

to explore the case in which the mass of the emitting atoms is much less than the mass of atoms of the foreign gas. In this case, one can use the simplest theory of collisional broadening of two-photon lines to fit the experimental data. On this basis we made a strong effort to study the collision of excited neon atoms with heavier atoms such as argon and krypton. Unfortunately, the rf discharge could last for only a very short time in these experiments, making it impossible to collect reliable data. However, this series of experiments can be performed with other atomic vapors such as sodium, for which the rf discharge is not necessary. In any case, our experimental results for He-Ne and Ne-Ne collisional broadenings and shifts of neon two-photon resonances may be used to calculate the repulsive and attractive parts of the interaction potential. For comparison, we have plotted the broadening and shift of Ne-Ne and He-Ne two-photon resonances in Figs. 8 and 9.
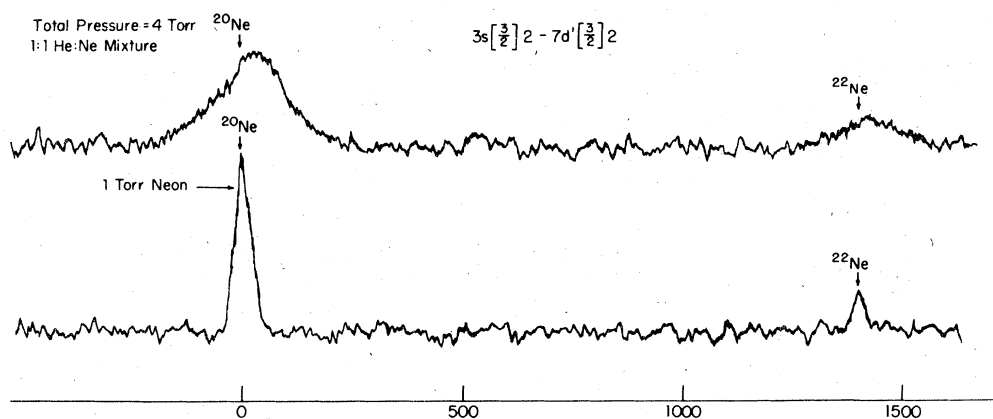
FIG. 7. Typical experimental trace for He-Ne collisions. The upper trace corresponds to the sample cell; the lower trace corresponds to the reference neon cell.
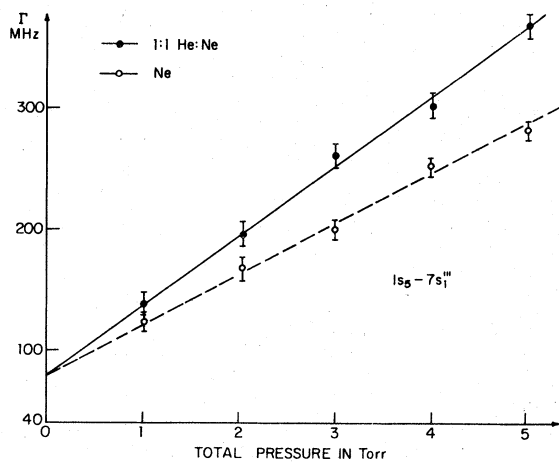
FIG. 8. He-Ne and Ne-Ne collision broadenings as a function of total pressure in the $1s_5$-$7s_1''$ two-photon transitions of neon.

VI. PHYSICAL DISCUSSION

These results demonstrate that the gathering of data characterizing the broadening and shift of the resonances to a high degree of accuracy presents no particular experimental difficulty. But the physical interpretation of collision processes and the selection of a theoretical model have proved to be difficult. Resonance shapes are affected by elastic angular scattering of atoms in collisons, by phase randomizing and quenching collisions, by the dependence of the line broadening and shift on atomic velocities, by resonant radiation trapping, by field polarization, and so on. The influence of so many factors makes it difficult to analyze experimental results, and presents problems for choosing a collision model and determining the constants characterizing elementary processes.

It is evident that in order to choose a collision model and obtain information about the constants of interaction, it is necessary to carry out a series of complex investigations, which may include the following experiments: (i) simultaneous measurements of the collisional broadening of a Doppler profile and of narrow resonances; (ii) the analysis of the narrow resonance shape and the Doppler profile of a line; (iii) investigation of "strong" collisions connected with resonance excitation exchange; (iv) research into line shift and collisional broadening; (v) investigation of the temperature dependence of broadening and shift; (vi) investigation of the dependence of line broadenings on a principal quantum number of one of the levels. Carrying out all of these investigations on one object presents a formidable task.

Finally, nonresonant forces are characterized by the dependence of the broadening on the relative velocity of colliding atoms. This dependence may be used to determine the type of interaction. Since the mean velocity of colliding atoms depends on temperature, the collisional broadenings and shifts are also functions of temperature.

This qualitative survey of collisional phenomena in two-photon spectroscopy is only an introduction to the complexity associated with the theoretical analysis. Certainly, a more accurate analysis of the observed spectra from our experiments is not possible without a great deal of knowledge about real collision models in two-photon spectroscopy. However, experimental results of the type discussed here could significantly contribute to the establishment of a solid basis for a more realistic
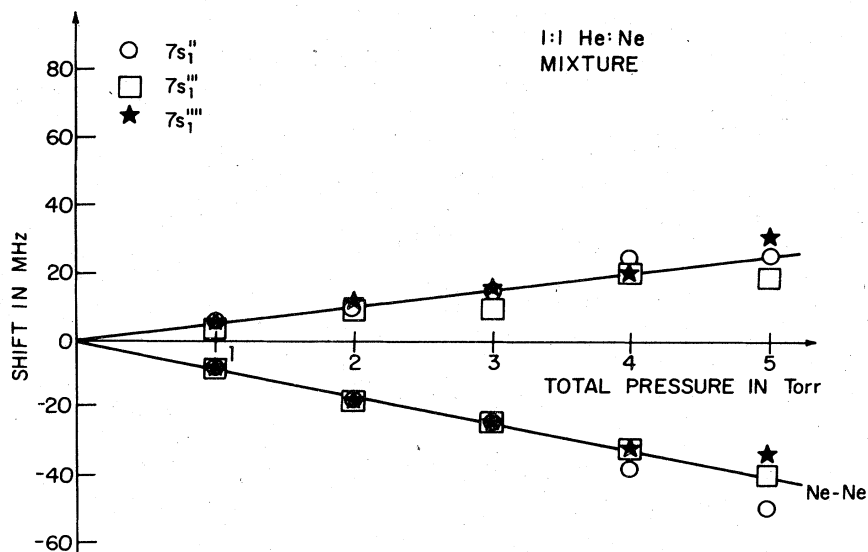
FIG. 9. He-Ne and Ne-Ne collisional shifts as a function of total pressure for the three two-photon transitions to subconfiguration $7d'$ of neon.

model applicable to various experimental situations.

ACKNOWLEDGMENTS

[1]S. Svanberg, P. Tsekeris, and W. Happer, Phys. Rev. Lett. 30, 817 (1973).

[2]S. Haroche, M. Gross, and M. P. Silvermann, Phys. Rev. Lett. 33, 1063 (1974); C. Fabre, M. Gross, and S. Haroche, Opt. Commun. 13, 393 (1975).

[3]L. S. Vasilenko, V. P. Chebotayev and A. V. Shishaev, Pis. Zh. Eksp. Teor. Fiz. 12, 161 (1970) [JETP Lett. 12, 113 (1970)]; B. Cagnac, G. Grynberg, and F. Biraben, J. Phys. (Paris) 34, 56 (1973); Phys. Rev. Lett. 32, 643 (1974); M. D. Levenson and N. Bloembergen, Phys. Rev. Lett. 32, 645 (1974); T. W. Hänsch, K. Harvey, G. Meisel, and A. L. Schawlow, Opt. Commun. 11, 50 (1974); M. M. Salour, Opt. Commun. 18, 377 (1976); J. P. Woerdman, Chem. Phys. Lett. 43, 279 (1976).

[4]The first of such experiments was performed by F. Biraben, E. Giacobino, and G. Grynberg, Phys. Rev. A 12, 2444 (1975), using a Rhodamine 6G cw dye laser to populate the $2p^54d$ and $2p^55s$ levels of neon [starting from $2p^53s$ $(J=2)$] at wavelengths very close to those of the 3^2S-4^2D and 3^2S-5^2S two-photon transitions in sodium.

[5]See, for example, B. DeComps, thesis (Paris, 1969) (unpublished); also G. Grynberg, thesis (Paris, 1976) (unpublished).

[6]G. Grynberg, thesis (Paris, 1976) (unpublished); also, J. Bauche, thesis (Paris, 1969) (unpublished); S. Liberman, thesis (Orsay, 1971) (unpublished).

[7]R. Wallenstein and T. W. Hänsch, Opt. Commun. 14, 353 (1975).

[8]F. Biraben, G. Grynberg, E. Giacobino, and J. Bauche, Phys. Lett. 56A, 441 (1976); E. Giacobino, F. Biraben, G. Grynberg, and B. Cagnac, J. Phys. (Paris) (to be published); also, G. Grynberg, thesis (Paris, 1976) (unpublished).

[9]M. M. Salour, thesis (Harvard, 1977) (unpublished); M. M. Salour, Opt. Commun. 18, 337 (1976).

[10]F. Biraben, B. Cagnac, and G. Grynberg, J. Phys. Lett. (Paris) 36, L-41 (1975); also P. R. Berman, Phys. Rev. A 13, 2191 (1976).